AIAA AVIATION Forum
June 25-29, 2018, Atlanta, Georgia
2018 Atmospheric and Space Environments Conference

10.2514/6.2018-3185



# Design of an Icing Wind Tunnel Contraction for Supercooled Large Drop Conditions

David M. Orchard[1], Krzysztof Szilder[2] and Craig R. Davison[3]
*National Research Council of Canada, Ottawa, Ontario, K1A 0R6, Canada*

**Various simulations of drop temperature and velocity are employed by wind tunnel facility operators with regards to SLD conditions. This paper compares several methods used in determining the level of thermal and momentum equilibrium of large drops and demonstrates the use of these as guidance for the design of a wind tunnel contraction that will provide simulation of SLD sprays consistent with those of the natural environment. For the current study, only freezing drizzle conditions where maximum drop diameter does not exceed 500μm was considered as this is consistent with the current SLD spray capabilities of most icing wind tunnels.**



## I. Nomenclature

| | | |
|---|---|---|
| Ac | = | Accumulation parameter |
| $\beta_0$ | = | Stagnation collection efficiency |
| $dV_{AIR}/dt$ | = | Air flow acceleration through the contraction, $m/s^2$ |
| $n_o$ | = | Freeze fraction |
| $T_{AIR}$ | = | Air temperature in test section, $^oC$ |
| $T_{DROP}$ | = | Drop temperature in test section, $^oC$ |
| $T_{SAT}$ | = | Static Air Temperature, $^oC$ |
| $V_{AIR}$ | = | Air velocity, m/s |
| $V_{DROP}$ | = | Drop velocity, m/s |
| X | = | Overall length of contraction, m |
| x | = | Streamwise location along wind tunnel contraction, m |
| $\Delta x$ | = | Streamwise increment in contraction length, m |

## II. Introduction

Until recently, the maximum icing envelopes used for the certification of transport category airplanes have been performed in accordance with the Title 14 Code of Federal Regulations (CFR) Part 25 Appendix C [1] that defines the icing environments with a median volume diameter (MVD) up to 40 μm for continuous maximum (stratiform clouds) and up to 50μm for intermittent maximum (cumuliform clouds). However, following the accident of an ATR-72 at Roselawn, Indiana in 1994, the National Transport Safety Board report [2] concluded that the 14 CFR Part 25 Appendix C icing envelope has limitations regarding certification in conditions that contain Supercooled Large Drops (SLDs) with diameters in excess of 100 μm.

In order to better understand the SLD environment, a series of international collaborative projects were conducted to measure and assess aircraft icing conditions that contain SLDs [3-9]. The data provided by these studies have led to a greater understanding of the icing environment and enabled the expansion of the icing certification requirements to encompass SLD conditions through addition of Appendix O to 14 CFR Part 25 [10].

In order to demonstrate compliance to updated icing certification that includes SLD conditions, manufacturers will have an increased need for access to test facilities that can simulate this environment. Many of the current test facilities used for development and certification of aircraft components in icing, however, have been developed considering the simulation of conditions defined by Appendix C of CFR Part 25. Anderson and Tsao [11] examined the application of recognized scaling parameters used for Appendix C conditions [12][13] to those into the SLD

[1] Senior Research Officer, Aerospace Research Centre, AIAA Senior Member.
[2] Senior Research Officer, Aerospace Research Centre
[3] Senior Research Officer, Aerospace Research Centre

regime and showed that, for MVDs up to 190μm, similar methodology does indeed lead to matching of the main ice shape and can, potentially, be used to address drop size limitations of icing wind tunnel facilities. These methods, however, were shown not to apply to the growth of large features (feathers) aft of the main ice shape at increased drop sizes and suggested further study is required to understand the physical mechanisms of feather accretion. These methods showed that matching the freeze fraction, $n_0$, and the product of stagnation collection efficiency and accumulation parameter, i.e., $\beta_0 Ac$, with constant velocity and model size [11] were important factors in scaling ice shapes at SLD conditions. These parameters are, however, influenced by drop trajectory ($\beta_0 Ac$) and energy balance ($n_0$) and at higher drop sizes, as drop velocity and temperature starts to deviate significantly from that of the surrounding air flow, applying the Appendix C scaling methods present a number of challenges. As a result, facilities will need to determine any deficiency in these quantities to consider their impact on simulating valid in-flight SLD conditions.

While drop velocity can be measured through optical techniques such as Particle Image Velocimetry (PIV), means of measuring drop temperature within a wind tunnel environment are difficult and many facilities opt to assess this through simulation alone.

Various simulations of drop temperature and velocity are employed by wind tunnel facility operators with regards to SLD conditions. The objective of this study is to compare some of the methods used in determining the level of thermal and momentum equilibrium of large drops and use these as guidance for the design of a wind tunnel contraction that would be necessary to provide simulation of SLD sprays without the need for scaling. For the current study, only freezing drizzle conditions where maximum drop diameter does not exceed 500μm are considered as this is consistent with the current SLD spray capabilities of most icing wind tunnels.



## III. Wind Tunnel Contraction Design

For this study, a hypothetical wind tunnel design has been considered that has a contraction ratio of 12:1 and a length of 9.1m (30ft) from the point of spray injection to entrance to the test section. The test section is a square profile with an area of 0.37m$^2$ (4ft$^2$). The contraction profile is shown in Fig. 1, and has been designed based on the approach of Stallabrass [14] considering an analytical variation of acceleration, *dV/dt*, along the nozzle centreline, expressed by the relationship,

$$\frac{dV}{dt} \propto sin^2 \frac{\pi x}{X} \tag{1}$$

where x is the streamwise distance from the contraction entry and X is the overall length of the nozzle.

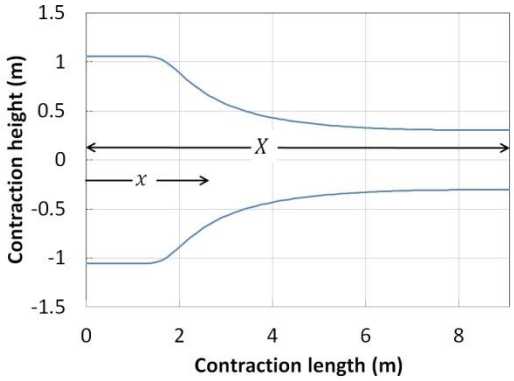


**Fig. 1 Wind tunnel contraction profile**

## IV. Drop Temperature and Velocity Analysis Tools

Four different analysis tools were used to predict the drop temperature and velocity throughout the contraction section. These were:

A. Arnold Engineering Development Center (AEDC) One Dimensional Multi-phase code (1DMP) [15][16]
B. NRC's droplet evaporation model [17]
C. Three Dimensional droplet trajectory and thermodynamics model (3D TT) [18]
D. NRC's Isokinetic Probe (IKP) evaporation model. [19]

Of these, the AEDC 1DMP code is the most widely used by facility operators when determining the level of thermal and momentum equilibrium of icing cloud conditions.

### A. AEDC 1DMP

This one dimensional code employs a mathematical model for the evaluation of aero-thermodynamics of multi-phase flow in a duct, based on the overall conservation of species, mass, momentum and energy [20]. Originally, this model used a single droplet diameter but was later extended to a multi-binned version to address issues with calculating low MVD values due to its inability to simulate evaporation of smaller water particles present in the spray profile [17]. This code is widely used by the aircraft icing test community to assess (and correct for) MVD and Liquid Water Content (LWC) changes due to evaporation between the spray mast and the test article. In addition, many wind tunnel facilities use the AEDC model to evaluate droplet velocity and temperature relative to ambient conditions.

### B. NRC's Droplet Evaporation Model

This code was developed to provide an online multi-binned evaporation model as part of the control system of engine test cells. By providing real-time calculation of MVD and LWC due to evaporation between the spray mast and test article, the code enables control of water flow rates and atomizing air pressure to maintain desired icing cloud conditions.

### C. Three dimensional droplet trajectory and thermodynamics model (3D TT)

The main principles of the droplet trajectory and thermodynamics model (3D TT) are described by Gates et al. [18]. It incorporates three main components: calculation of the flow field, determining the drop trajectory and analysis of heat exchange between the drop and air temperature. Unlike the process described in [18], the flow field for the wind tunnel contraction provided in Fig. 1 was calculated via CFD and the solution used to provide flow profiles for calculation in the trajectory model. For this trajectory model, the droplet is considered a solid sphere acted upon by gravity and drag force. To determine the drop temperature, the thermodynamic model equates the rate of change of the internal energy of the drop to the net heat transfer into the airstream due to convection and evaporation.

### D. NRC IKP

A one dimensional code that was originally developed to simulate the evaporation of water droplets passing through an isokinetic probe. This is a single binned model that calculates heat transfer in the flow path along with directional changes due to the velocity field. Gravity is included in the calculations as are phase changes from ice to liquid to vapour [19].

## V. Simulation Conditions

For these simulations, a monodispersed drop (single binned) distribution was "injected" in the settling chamber at a streamwise distance of x = 0 using 10 different drop diameters from 20μm to 500μm. The drop sizes along with the wind tunnel operating conditions used during the simulations are given in Table 1.

**Table 1 Simulation conditions in test section**

| Parameter | Value | Unit |
|---|---|---|
| Air Velocity | 105 | m/s |
| Initial Water Temperature | 10 | $^{o}$C |
| Air Total Temperature | -10 | $^{o}$C |
| Air Static Temperature | -15.6 | $^{o}$C |
| Air Relative Humidity | 80 | % |
| Stagnation Pressure | 98,000 | Pa |
| Static Pressure | 92,068 | Pa |
| Liquid Water Content | 0.5 | g/m$^3$ |
| Initial Water Drop sizes[4] (at x = 0) | 20, 40, 80, 120, 160, 200, 250, 300, 400, 500 | μm |

## VI. Drop Temperature and Velocity Code Comparison

Drop temperature obtained from the AEDC 1DMP code and 3D TT model (500μm case only), along the centerline of the wind tunnel contraction, is provided in Fig. 2 and demonstrates close comparison is achieved between both methods. As expected, with increasing diameter, the drop temperature at the entrance to the test section increases. For the largest diameter simulated (500μm), drop temperature is approximately 10$^{o}$C warmer than the tunnel airflow. The difficultly in providing an appropriate contraction design for larger drop conditions is also emphasized when considering the velocity profiles as shown in Fig. 3. Here, as a result of increased drag on the larger drops, the difference in velocities between the freestream and 500μm drop is approximately 20m/s. As with the temperature field profiles, there is also close agreement in the drop velocities provided by the two methods. It should be noted that for the AEDC 1DMP and 3D TT simulations, deformation due to shear forces is not considered and the drag force is calculated assuming drops retain a spherical shape throughout the contraction length.

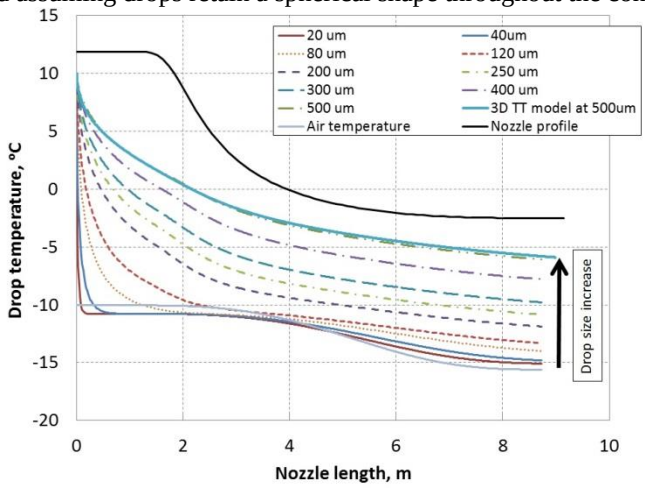


**Fig. 2 Temperatures of drops with diameters up to 500μm throughout wind tunnel contraction from the AEDC 1DMP and 3DTT analysis**

[4] These are the drop diameters at the location of spray injection; mass loss due to evaporation throughout the contraction results in smaller diameters at the test section location

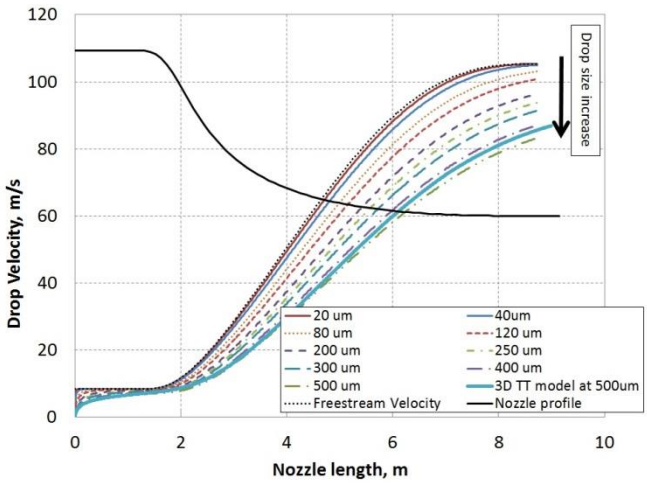


**Fig. 3 Velocity of drops with diameters up to 500µm throughout wind tunnel contraction from the AEDC 1DMP and 3DTT analysis**

The NRC's droplet evaporation and IKP evaporation models were also used to compute the drop temperature and velocity at the test section entrance and compared to output from the AEDC 1DMP simulation. The difference between drop temperature and velocity compared to that of the freestream from these three codes is given in Fig. 4 and indicates close comparison of temperature and velocity difference across the range of drop sizes analyzed.

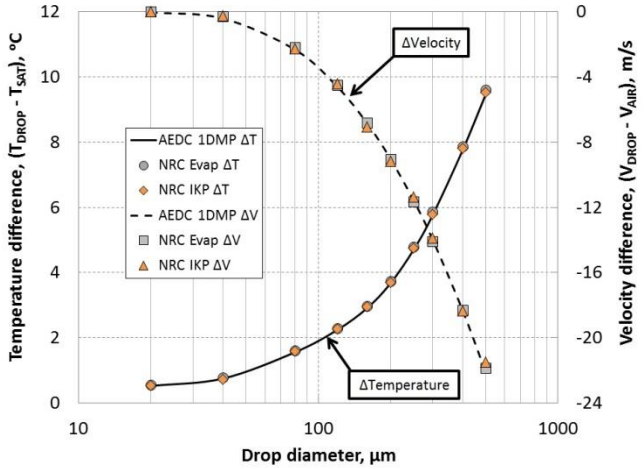


**Fig. 4 Comparison of drop temperature and velocity at the test section entrance from AEDC 1DMP, NRC's droplet evaporation and IKP evaporation models.**

In addition to the differences between drop and wind tunnel flow conditions, large drops are also prone to gravitational settling resulting in either an impact with the wind tunnel floor or stratification of the spray distribution in the test section, with the larger drops tending to be distributed closer to the tunnel floor. The drop trajectory provided by the 3D TT model enables the level of gravitational settling to be simulated. This is demonstrated in Fig. 5 showing the 500µm drop trajectories from the spray bar location to the test section for two different test section velocities, i.e., 105m/s and 52.25m/s. For the 105m/s velocity, the drops are concentrated into the lower half of the test section, with a small amount of drops impacting the wall and floor of the contraction section immediately downstream of the settling chamber (in the figure, drop/wall impact is indicated by a sphere). For the lower air velocity, however, the number of drops that impact with the contraction section increases and the spray that gets through the contraction is more concentrated closer to the test section floor. In this figure, the drop temperature throughout the contraction is also indicated via colour coding of the drop trajectories, e.g., the red spheres indicates an initial drop temperature of 10$^{o}$C, whereas for the 105m/s test section velocity, green spheres at the end of the

trajectory indicate a drop temperature of approximately -6°C. The drop temperature for the lower velocity, however, is closer to that of the air velocity as a result of the increased residence time.

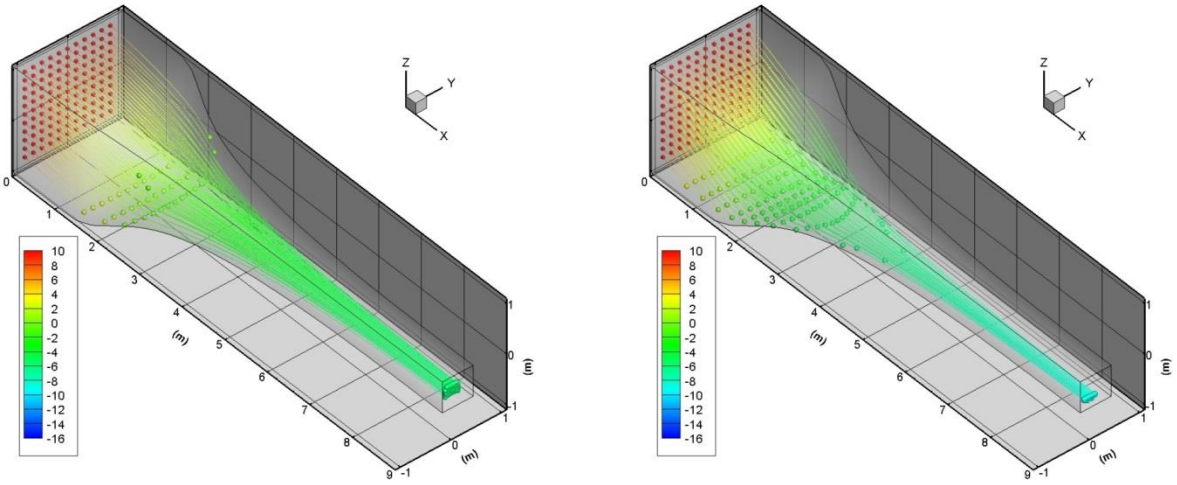


a) 500µm diameter drop trajectories at 100% freestream velocity

b) 500µm diameter drop trajectories at 50% freestream velocity

**Fig. 5 Drop trajectories and temperatures for 500µm diameter drops at 100% and 50% freestream velocity. Spheres indicate initial and final locations with colour providing drop temperature.**

The amount of drop/wall impact and the test section distribution is also shown in Fig. 6, which provides a downstream view of drop trajectories for three diameters (20µm, 250µm and 500µm) and two velocities (105m/s and 52.25m/s). For the 20µm drops, an even spray distribution is provided for both velocities and no wall impact is observed. As the drop sizes increase to 250µm, however, the spray distribution is more concentrated towards the lower half of the test section and there is some impact with the contraction. The concentration in the test section, as well as the amount of wall impact, increases as the velocity reduces. This becomes more evident when drop diameter is increased to 500µm resulting in a concentrated spray distribution close to the test section floor combined with an increase in impact of drops with the contraction. As with Fig. 5, Fig. 6 also has colour coding of the drop trajectories and shows that improved temperature equilibrium is achieved at the lower velocities as a result of the increased residence time.

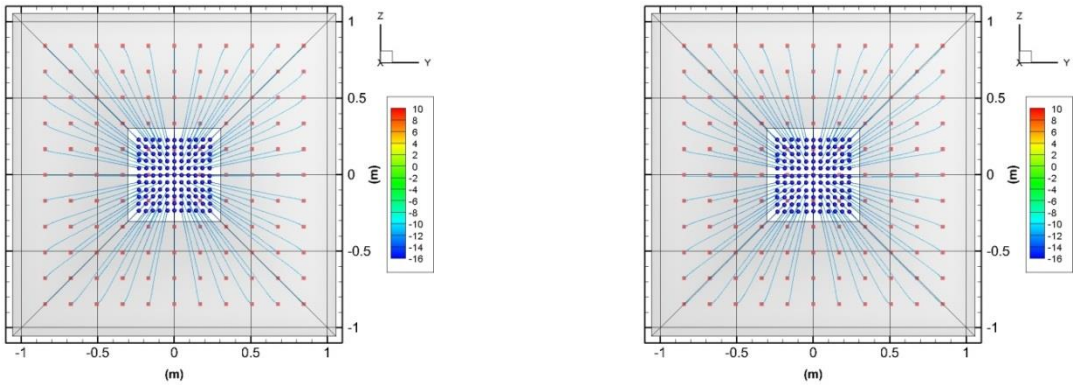


a) 20µm drop at 100% freestream velocity

b) 20µm drop at 50% freestream velocity

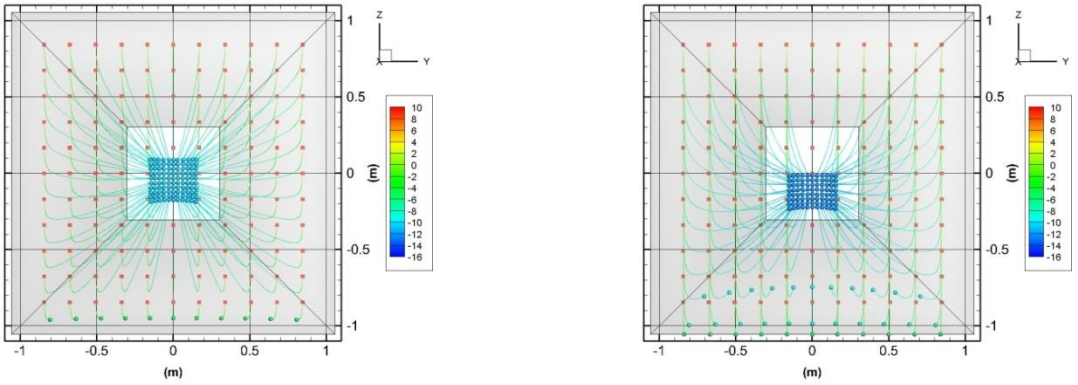

c) 250µm drop at 100% freestream velocity d) 250µm drop at 50% freestream velocity

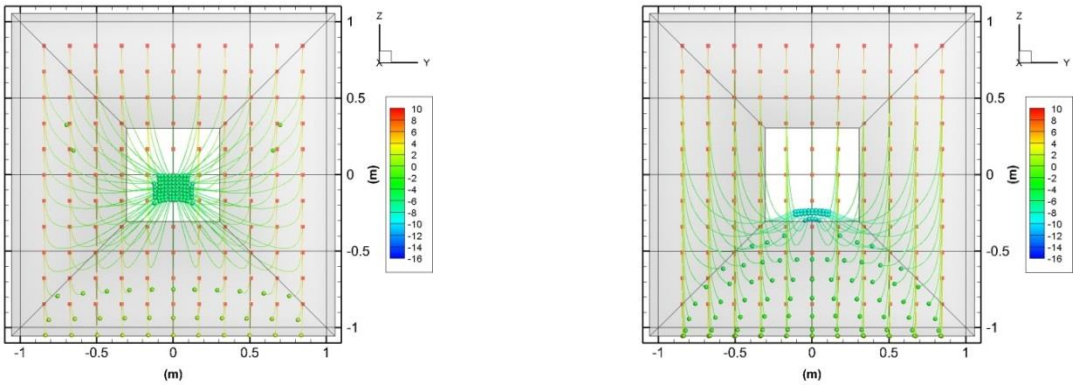

e) 500µm drop at 100% freestream velocity f) 500µm drop at 50% freestream velocity

**Fig. 6 Drop trajectory and temperature (looking downstream from settling chamber). Red dots indicate initial drop temperature, i.e., 10°C**

## VII. Designing a Wind Wunnel for SLD Freezing Drizzle Conditions

As shown in the analysis of the hypothetical wind tunnel contraction design, for drop sizes that extend into those expected for SLD freezing drizzle conditions, consideration of the distance between the spray injection and test article needs to be made if both thermal and momentum equilibrium with the surrounding airflow is to be achieved. To assess a contraction design that would satisfy this requirement, the AEDC 1DMP has been combined with a MATLAB routine that modifies the contraction section length until momentum and thermal equilibrium is achieved. The flow chart given in Fig. 7 provides the structure of the MATLAB routine. Here, the flow conditions and drop diameters are as given in Table 1, and the same contraction and test section areas of the hypothetical wind tunnel design, described in section III are defined. The wind tunnel contraction coordinates are then calculated using the contraction profile provided from equation 1. The MATLAB routine then writes the necessary input files and executes the AEDC 1MP code. The resulting drop temperature and static temperature at the entrance to the test section are acquired from the AEDC output files and, if the drop temperature is greater than 5% of the tunnel static temperature, the length of the contraction is increased by $\Delta x$ (0.6m) and the process repeated. Once the temperature condition is satisfied, the same approach is applied to the difference between the drop velocity and tunnel velocity. Once both temperature and velocity are within 5% of the tunnel conditions, the analysis is stopped and the contraction length and profiles for a particular drop size are obtained.

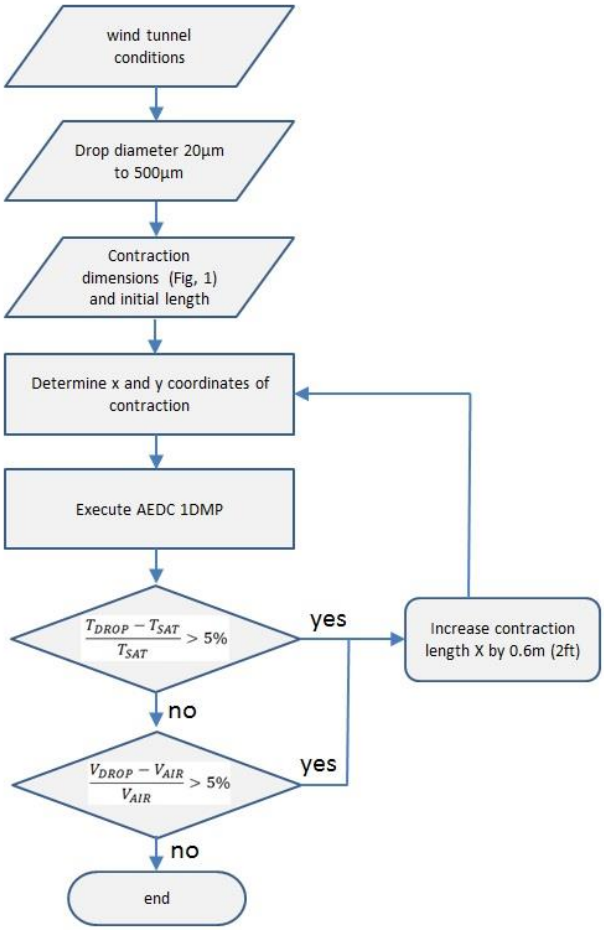


**Fig. 7 MATLAB SLD nozzle design flowchart**

The nozzle profiles obtained from this routine are shown in Fig. 8 along with the length of the contraction needed to satisfy thermal and momentum equilibrium for the -10°C total temperature conditions in Fig. 9. The AEDC 1MP code indicates that the contraction length needs to be extended as the drop size increases to allow for sufficient residence time to cool the drops. For the particular wind tunnel conditions and nozzle geometry used in this analysis, with a drop diameter of 500µm, the nozzle length would need to extend close to 130m for this to be achieved. This is, obviously, not only a function of the nozzle geometry and drop size, but also one of the flow temperature and velocity. To demonstrate this, the AEDC 1DMP analysis has been conducted with the freestream total temperature decreased from -5 to -25°C for drop diameters from 100µm to 500µm. Fig. 9 shows the contraction lengths required to obtain momentum and thermal equilibrium increases up to 175m for the 500µm diameter drops at a total temperature of -25°C.

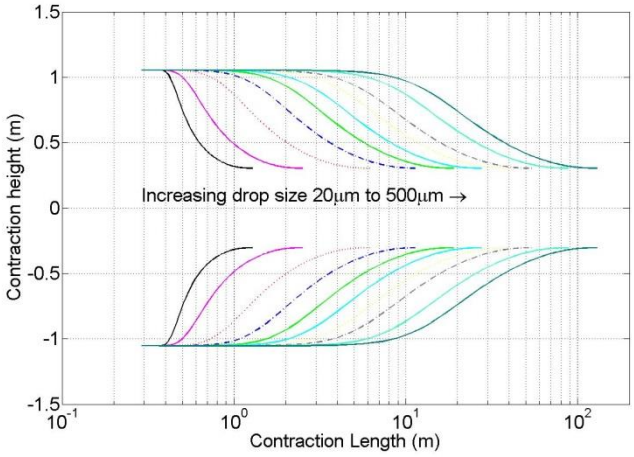


**Fig. 8 Nozzle profiles for thermal and momentum equilibrium for drop sizes from 20 to 500μm**

The simulation of drop temperature, velocity and trajectory highlights the challenges of providing natural supercooled large drop conditions in traditional icing wind tunnel. Any facility capable of achieving this may need to be prohibitively large to provide sufficient residence time for thermal and momentum equilibrium. In addition, such a facility would likely have to have a vertical test section to maintain adequate spray distribution. It should also be noted that the simulations highlighted here are restricted to freezing drizzle, where maximum drop diameters are less than 500μm. Extending this for freezing rain conditions, where drop diameter can extend to over 1mm, would further compound the problem of achieving adequate simulation of natural SLD conditions.

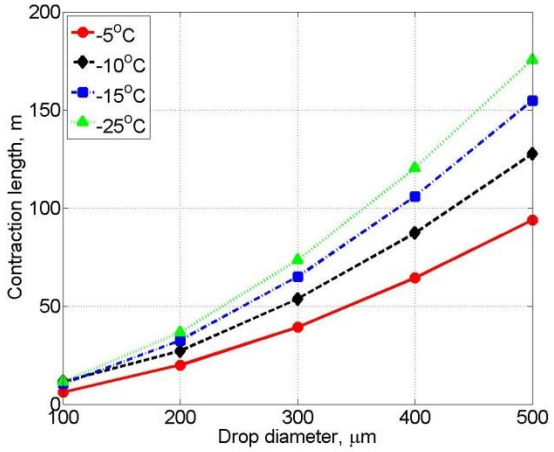


**Fig. 9 Nozzle length requirements for thermal and velocity equilibrium of drops up to 500μm with various total temperature**

## VIII. Conclusion

Close comparison in both drop temperature and velocity has been observed using four separate simulation methods (AEDC 1DMP, NRC's droplet evaporation model, 3D droplet trajectory and thermodynamics model (3D TT) and NRC's IKP droplet evaporation model) over a range of drop sizes as they pass through a wind tunnel contraction section. It is shown that for a contraction length of 9.1m (30ft) and test section velocity of 105m/s, there is insufficient residence time to attain thermal and momentum equilibrium between the flow and the larger drop diameters. Indeed, for the largest diameter (500μm), drop temperature and velocity differed from that of the freestream conditions by 10°C and 20m/s respectively.

Drop trajectories obtained from the 3D TT model show that larger drops are subject to gravitational settling, leading to stratification of the mass distribution in the test section and some drop impingement with the wind tunnel

floor and walls. The spray stratification and wall impingement is seen to increase as the freestream velocity is reduced.

Through the use of the AEDC 1DMP code combined with a MATLAB routine, it was possible to calculate the necessary contraction length to attain drop temperature and velocity equilibrium for drop sizes from 20μm to 500μm. This was done using the same contraction ratio and test section areas defined for the hypothetical wind tunnel contraction, i.e., 12:1 and $0.37m^2$. For the wind tunnel contraction profile and drop sizes analyzed, for equilibrium to be achieved, the contraction length varies from 1.3m for a 20μm diameter drop up to 130m for a 500μm diameter drop. As the tunnel temperature reduces, the length required to attain equilibrium conditions extends further still.

While drop temperatures and velocities need to be validated through experimental methods, the close comparisons obtained between the four separate codes provides a level of confidence in the ability to predict spray conditions for freezing drizzle SLD and demonstrates that drop residence time may be prohibitively large to enable simulation of natural SLD conditions in traditional icing facilities. The implications of slower and warmer drops (compared to the freestream) on ice accretion of critical aircraft components will need to be examined along with effects of drop distribution and trajectory in the test section.



## IX. References


[1] Federal Aviation Administration, 1999, "Part 25: Airworthiness Standard: Transport Category Airplanes, Appendix C. Title 14: Aeronautics and Space, U.S., Code of Federal Regulations".

[2] National Transportation Safety Board, "In-Flight Icing Encounter and Loss of Control Simmons Airlines, d. b. a. American Eagle Flight 4184 Avions de Transport Regional (ATR) Model 72-212, N401AM, Roselawn, Indiana", NTSB/AAR-96/01, 1994.

[3] Miller, D., Ratvasky, T., Bernstein, B., McDonough, F. and Strapp, J.W., " NASA/FAA/NCAR Supercooled Large Droplet Icing Flight Research: Summary of Winter 96-97 Flight Operations", Proc. AIAA 36th Aerospace and Science Meeting and Exhibit, Reno, NV, AIAA 1998-0577, 1997.

[4] Curry, J.A., Hobbs, P.V., King, M.D., Randall, D.A., Minnis, P., Isaac, G.A., Pinto, J.O., Uttal, T., Bucholtz, A., Cripe, D.G., Gerber, H., Fairall, C.W., Garrett, T.J., Hudson, J., Intrieri, J.M., Jakob, C., Jensen, T., Lawson, P., Marcotte, D.L., Nguyen, L., Pilewskie, P., Rangno, A., Rogers, D.C., Strawbridge, K.B., Valero, F.P.J., Williams, A.G. and Wylie, D., 2000, " FIRE Arctic Clouds Experiment", Bulletin of the American Meteorological Society, 81, 5-29.

[5] Cober, S.G., Isaac, G.A. and Strapp, J.W., 2001, "Characterisation of Aircraft Icing Environments that Include Supercooled Large Drops", Journal of Applied Meteorology, Volume 40, 1984-2002.

[6] Cober, S.G. and Isaac, G.A., 2012, "Characterization of Aircraft Icing Environments with Supercooled Large Drops for Application to Commercial Aircraft Certification", Journal of Applied Meteorology and Climatology, Volume 51, 265-284.

[7] Cober, S.G., Bernstein, B, Jeck, R., Hill, E., Isaac, G., Riley, J. and Shah, A., 2009, "Data and Analysis for the development of an Engineering Standard for Supercooled Large Drop Conditions", U.S. Department of Transportation Final Report, DOT/FAA/AR-09/10.

[8] Isaac, G.A., Cober, S.G., Strapp, J.W., Korolev, A.V., Tremblay, A. and Marcotte, D.L., 2001a, "Recent Canadian Research on Aircraft In-flight Icing", Canadian Aeronautics and Space Journal, Volume 47, No.3.

[9] Isaac, G.A., Cober, S.G., Strapp, J.W., Hudak, D., Ratvasky, T.P., Marcotte, D.L. and Fabry, F., 2001b, "Preliminary Results from the Alliance Icing Research Study (AIRS)", Proc. AIAA 39th Aerospace and Science Meeting and Exhibit, Reno, NV, AIAA 2001-0393.

[10] Federal Aviation Administration, "Part 25: Airworthiness Standard: Transport Category Airplanes, Appendix O, Admt 25-140. Title 14: Aeronautics and Space, U.S., Code of Federal Regulations", 2014.

[11] Anderson, D.N. and Tsao, J-C, "Ice Shape Scaling for Aircraft in SLD Conditions", U.S. Department of Transportation Final Report, DOT/FAA/AR-07/55.

[12] Anderson, D.N., "Manual of Scaling Methods", NASA/CR-2004-212875, March 2004.

[13] Ruff, G.A., "Analysis and Verification of Icing Scaling Equations", AEDC-TR-85-30, vol 1(rev), March 1986.

[14] Stallabrass, J.R., "Feasibility Study – High Speed Icing Wind Tunnel Modifications", NRC report LT-179, January 1980.

[15] Schulz, R.J. "Second Report for Research and Modelling of Water Particles in Adverse Weather Simulation Facilities", AEDC TASK report 97-03.

[16] Schulz, R.J. "A Model for Predicting Mixed-Phase Flow in Ground Test Facilities", 37th AIAA Aerospace Sciences Meeting and Exhibit, AIAA 99-0308, January 1999, Reno, NV.

[17] Davison C.R., MacLeod J.D. and Chalmers J.L.Y., "Droplet Evaporation Model for Determining Liquid Water Content in Engine Icing Tunnels and Examination of the Factors Affecting Liquid Water Content", 9th AIAA Atmospheric and Space Environments Conference, AIAA 2017-4246, June 2017, Denver, CO.

[18] Gates E.M., Lam W. and Lozowski E.P., "Spray Evolution in in Wind Tunnels", Cold Regions Science and Technology, vol 15 (1), February 1988, pp 65-74.

[19] Davison, C.R., Landreville, C., Mings, V. and Currie, T.C., " Phase 2 Development and Testing of Isokinetic Probe to Measure Total Water Content During Ground and Airborne Testing", National Research Council, LTR-GTL-2014-0004, Ottawa, March 2014.

[20] Stallabrass, J.R., "Procedure for Allowing for Evaporation from Water Droplets in an Engine Icing Test Cell", National Research Council, LTR-LT-129, January 1982.